JOURNAL OF OPTOELECTRONICS AND ADVANCED MATERIALS Vol. 9, No. 7, July 2007, p. 2162 - 2165

Generation of oxide nanoparticles via femtosecond laser ablation

SUN QI[a,*], NI XIAOCHANG[a,b], LI HAIYAN[c], WANG CHING-YUE[a], CHAI LU[a], YANG LI[a], JIA WEI[a]
[a]*Key Laboratory of Optoelectronic Information Technical Science, EMC; Ultrafast Laser Laboratory, School of Precision Instruments and Optoelectronics Engineering, Tianjin University, Tianjin 300072, China*
[b]*Electronic Engineering Department, Tianjin University of Technology and Education, Tianjin 300222 , China*
[c]*Electronic Information School, Tianjin University, Tianjin 300072, China*

Oxide nano-particles have some important applications, so the possibility to generate oxide nano-particles was provided on some solid material via femtosecond laser in atmosphere. Experimental results present that nanoparticles' size distribution and average size can be directly controlled by laser fluences and pulse numbers. Femtosecond laser ablation can be an efficient process to produce oxide nano-particles around the irradiated area on some solid materials in atmosphere

(Received April 11, 2007; accepted June 27, 2007)

Keywords: Femtosecond laser, Nanoparticles, Microstructure fabrication, Pulse laser deposition

1. Introduction

Oxide nano-particles (ONPs) such as ZnO, CuO, Ni_2O and Al_2O_3, have been attracting increasing interest for their superior physical and chemical characteristics which have potential applications in micro optoelectronic devices [1,2] and active catalysts. Many conventional techniques, for example, electrochemical electrochemical deposition [3], vapor deposition [4], and arc discharge [5] are effective for ONPs's generation, however, these traditional methods usually have some disadvantages such as impurity, porosity and wide size distribution.

With the development of laser micromachining [6], pulsed laser ablative deposition (PLD) with a solid target has been utilized to gain thin films as well as NPs and their aggregates. Now, more and more researchers have focused attention on the possibility to generate NPs via PLD especially the PLD of femtosecond (fs) laser pulses, because it may overcome many limitations in the traditional techniques mentioned above [7,8]. Comparing with longer pulses (ns or ps time scale), the period of fs pulses acting with targets is staggered with the period of ejecting, which avoids the complicated secondary laser interactions. Moreover, fs laser pulses can heat solid materials to get much higher temperature and pressure, meanwhile with much lower fluence before significant thermal conduction happens. It suggests that any material can be heated to solid density plasma. Significantly, with precise low threshold, the ablation process and corresponding results are controllable.

As we know, non-oxidative NPs are always produced [9] in a cavity with some extreme conditions and assistant devices, such as ambient gas or vacuum, controlled pressure and temperature, and paralleled machining desk. However, the generation of ONPs via fs laser ablation doesn't need any additional assistant conditions and devices, the sufficient oxidation process can be directly achieved during the fs laser ablation around the irradiated area on the solid material in atmosphere, notably, the distribution and the average size of ONPs can be controlled by laser fluences and pulse numbers.

2. Experimental

The experiment is executed with an amplified solid-state Ti:sapphire laser micromachining system (UMW-2110i, Clark-MXR Inc.), providing 150fs pulse duration, 775 nm central wavelength, 1 kHz repetition rate, and various output energy from 0 to 1mJ per pulse. The laser beam approximates to a Gaussian shape for intensity spatial profile. Targets were mounted on orthogonal XYZ stages, (accuracy X Y: 10 nm, Z: 1.0 μm). A 5×objective was mounted on z stage, and the laser beam radius on focal scale is approximately 11 μm. All the progress can be controlled through the computer.

As Fig. 1 showed, plasma was evaporated to the atmosphere after irradiated by fs laser at normal incidence, followed by NPs' appearance in and around the ablated areas on the surface. The results were characterized by an AFM (atomic force microscopy) and SEM (Scanning electron microscope). Si (111), Al and Ni were drilled at the same laser fluence with increasing pulse numbers. And different fluence was also utilized to compare the results. Al and Ni are slices around several microns thick.

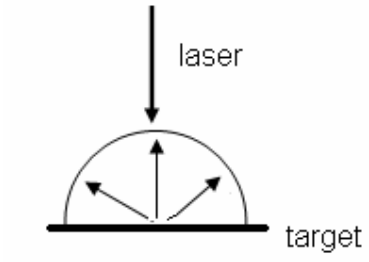

Fig. 1. Model of micromachining.

3. Results and discussion

Eliezer and Eliaz's [10] theoretical research has explained that NP's generation in vacuum from solid targets may involve different mechanisms, including liquid phase ejection, fragmentation, homogeneous nucleation and decomposition, etc. [11,12].

In ideal conditions (in vacuum and adiabatic condition), first, the laser energy is deposited in the electron subsystem, within few tens of nanometers thick of the surface layer. After the pulse ends and before the hydrodynamic expansion begins, the electrons in the surface layer undergo cooling by heat diffusion and heat transfer to ions (phonons). The electron temperature (*Te*), ion temperature (*Ti*), and absorption coefficient *A* are calculated from energy conservation equations in Ref. 13, applying the Helmholtz equation. This heat transfer stage continues for several picoseconds, and at the equilibrium (*Te*=*Ti*) state, we get the initial conditions for the adiabatic plasma expansion.

Next, the expansion starts presenting in plume form with large numbers of atoms, ions and molecules etc. When the fluence increases, micro burst blows off sub micron particles. NPs' dynamics in fs PLD [14] is provided by following the emission spectrum, which finally proves that laser fluence plays a primary role in NPs' generation.

Considering the background atmosphere, chemical reaction also happens. These particles collide with the air molecules, and react with oxygen, cooling down for the background resistances such as temperature, pressure and collisions. And the other reason for ONP's redeposition is direct air breakdown near the irradiated area [15]. The ionization of the ambient gas during fs laser pulses can generate a high-pressure plasma layer near the target surface after the termination of femtosecond laser pulse, which can restrain the expansion of the ablated material. Thereby the redeposition of the ablated material is enhanced. Finally, ONPs redeposit on the target.

As Fig. 2 shows, after femtosecond laser ablates Al, Ni and Si(111), NPs appear in and around the drilled area. Fig. 3 details the profile of NPs around the irradiated place in Fig. 2 (h). Each target in Fig. 2 is micromachined at laser fluence Φ_0=0.23 J/cm^2 with increasing pulse number N=100,200, and 500. It can be concluded that NPs are generated in and around the fabricated place, and the quantity of NPs increase significantly when the pulse number N goes up at the same Φ_0.

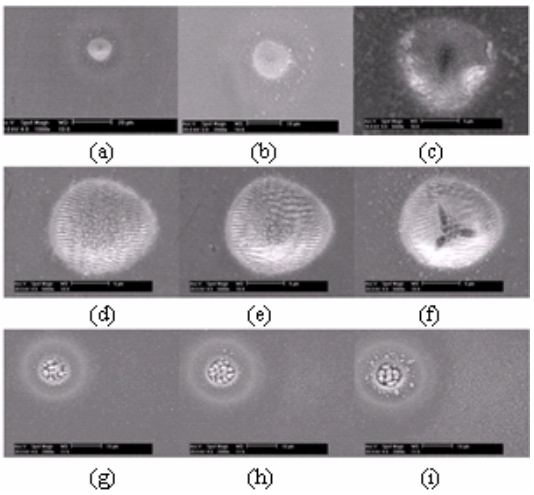

Fig. 2. NPs on Al, Ni and Si(111) at Φ_0 =0.23J/cm^2. (a)-(c) Al (d)-(f) Ni (g)-(f) Si(111); (a) (d) (g)N=100, (b) (e) (h) N = 200, (c)(f)(i)N=500.

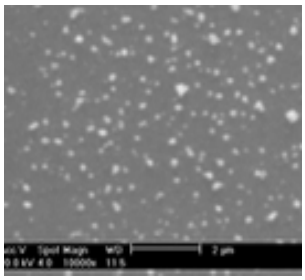

Fig. 3. Details of ONPs in fig. 2 (h) on Si(111).

All the NPs generated are oxidated on different materials. Fig.4 shows the spectrum charts of NPs around the irradiated areas on Al, Ni, and Si(111) targets, which are evidently oxidated. Corresponding to Fig. 4, the concrete oxide percentages of the ONPs are listed in Table 1. Considering the oxygenic ratios, the oxidation of NPs on Al, Ni and Si(111) is limited to a surface layer. This issue indicates that the oxide in NPs does result from oxidation of elemental NPs in contact with ambient air, which means the oxide happens after non-oxidative NPs formed.

Table 1. The oxide percentage of the ONPs corresponding to Fig. 4.

Elements	Al		Ni		Si(111)	
	Al K	O K	Ni K	O K	Si K	O K
Weight percentage	93.49	6.51	90.17	9.83	88.42	11.58
Atom percentage	89.48	10.52	71.44	28.56	81.31	18.69
Total	100.00		100.00		100.00	

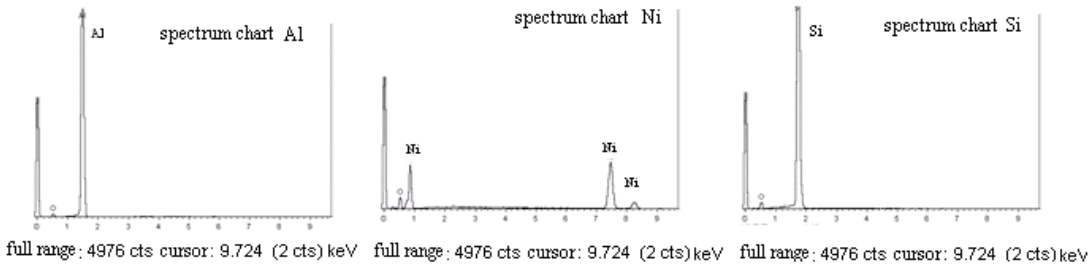

Fig. 4. Spectrum Chart of NPs' on Al, Ni, and Si(111) targets.

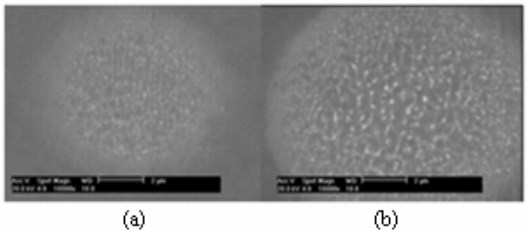

Fig. 5. NPs on Ni (N=10).

Focusing on one target, Ni for example (Fig. 5), which is fabricated at 0.116 J/cm^2 in (a) and 0.23 J/cm^2 in (b) when N=10. It is easy to notice that the NPs' sizes (both enlarged to 10000 times with SEM) are smaller in (a) than that in (b). This happens on every target, and the figures of average diameters of NPs around the illuminated place are listed from AFM in Table 2.

Table 2. Particles' average size (nm). Laser fluence Φ_0 (J/cm^2);Pulse number N.

Φ_0 \ N		10	100	200	500
Ni	0.23	0	75.7	85.8	91
	0.116	49.7	64	72.3	85.6
Al	0.23	70.9	77.5	87.7	96
Si(111)	0.23	0	76	87	93.2

Actually, all of them perform the same way when N increases from 10 to 500. The particle numbers rise significantly with N at the same fluence but the diameters of NPs do not. Fig. 6 figures out the trend of the changing diameters: (i) NPs' size presents insensitive when material changed at the same fluence. (ii) There is no big size growth if only N mounts up. (iii) Remarkable decrease of diameter happens when Φ_0 is reduced. (ix) Sub-micron particles appear on the edges when more energy deposits. All have agreements with the theory above that laser fluence is the key parameter.

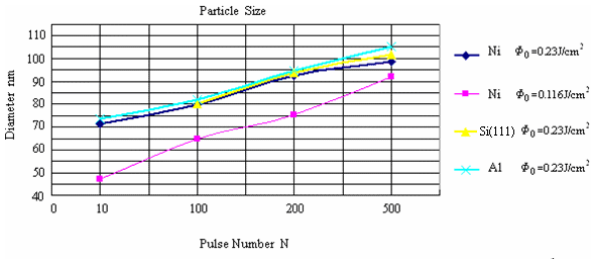

Fig. 6. Diameters' changing trend. Average diameters on different targets at 0.116J/cm^2, 0.23J/cm^2 when N increases

NPs appear symmetrically around the ablated center as Fig. 2 showed, that provides an evidence of plasma's axial symmetry. The size distribution is around 20 nm, and will be bigger while N increases. Ni for example, when Φ_0 =0.23J/cm^2, the distribution is listed in Table 3.

Table 3. Size distribution of Ni when Φ_0 =0.23J/cm^2.

N	10	100	200	500
Ni (nm)	60-78	62-83	69-88	70-99

Unlike PLD in cavity where many NPs enter the atomic layer of the substrate's surface, most of ONPs in our experiment are removable, and can be easily displaced from the solid board. It means that the board material will not disturb the following applications of ONPs.

Further investigation about the chemical and physical properties of generated ONPs via fs laser should be on schedule. And we expect that the nonoxidation experiments should be validated by a ventilated set with N_2 or Ar flow to get pure non-oxidative NPs, which may deeply low down the cost of NPs' production.

4. Conclusion

A practical way to produce ONPs via fs laser micro-fabrication was executed through this experiment. As the experimental results proved, it is a fast reaction

process, and has controllable sizes and a narrow size distribution. Considering the extensive application of ONPs, we think this technique has a promising application of laser chemical on different materials by intense fs laser pulses in the future.

Acknowledgement

This work was supported by the Key Grant Project of Chinese Ministry of Education (No.10410), by national scientific fund (N0. 606008004), by the Tianjin University of Technology and Education Fund (No.KYQD06001), and by the Science and technology development project fund of Tianjin city (No.043103911).

References

[1] H. Kim, C. M. Gilmore, J. S. Horwitz, A. Piqué, H. Murata, G. P. Kushto, R. Schlaf, Z. H. Kafafi, D. B. Chrisey, Appl. Phys. Letter, v76 (2000).
[2] Junji Kido, Hiromichi Hayase, Kenichi Hongawa, Katsutoshi Nagai, and Katsuro Okuyama, Appl. Phys. Letter, **65** (1994).
[3] S. Banerjee, S. Roy, J. W. Chen, D. Chakravorty. J. Magn. Magn. Mater. **219**, 45 (2000).
[4] S. L. Stoll, E. G. Gillan, A. R. Barron, Chem. Vap. Deposition. **2**, 182 (1996).
[5] Lozovik, Yu. E., A. M. Popov, Mol. Mate. **7**, 89 (1996).
[6] N. Rizvi, D. Milne, P. Rumsby, M. Gower, in Proceedings of Laser Applications in Microelectronic and Optoelectronic Manufacturing V, 24-26 Jan. 2000, San Jose, CA, USA.
[7] X. Liu, D. Du, G. Mourou, Laser Ablation and Micromachining with Ultrashort Laser Pulses, IEEE Journal of quantum electronics. **33**(10) (1997).
[8] E. G. Gamaly, A. V. Rode, B. Luther-Davies, Physics of plasmas. **9**(3), 949-957 (2002).
[9] S. Amoruso, G. Ausanio, R. Bruzzese, M. Vitiello, X. Wang, Phys. Rev. B **71**, 033406 (2005).
[10] S. Eliezer, N. Eliaz, E. Grossman, D. Fisher, I. Gouzman, Z. Henis, S. Pecker, Y. Horovitz, M. Fraenkel, S. Maman, Y. Lereah, Phys. Rev. B **69**, 144119 (2004).
[11] T. E. Glover, J. Opt. Soc. Am. B **20**, 125 (2003).
[12] D. Perez, L .J. Lewis, Phys. Rev. **B67**, 184102 (2003).
[13] D. Fisher, M. Fraenkel, Z. Henis, Phys. Rev. B **65**, n1 (2002).
[14] S. Amoruso, R. Bruzzese, N. Spinelli, R. Velotta, M. Vitiello, X. Wang, Appl. Phys. Letter **84**(22): 4502-4 (2004).
[15] A. Y. Vorobyev, Chunlei Guo, in Proceedings of LFNM 2006. 8th International Conference on Laser and Fiber-Optical Networks Modeling (IEEE Cat. No.06TH8874), 39-41 (2006).

*Corresponding author: sqwater@gmail.com